Available online at www.sciencedirect.com
SCIENCE DIRECT®
Journal of Sound and Vibration 279 (2005) 217–235
JOURNAL OF SOUND AND VIBRATION
www.elsevier.com/locate/jsvi

Coupled vibration analysis of liquid-filled rigid cylindrical storage tank with an annular plate cover

Young-Wann Kim[a,*], Young-Shin Lee[b]

[a] *Department of Mechanical Engineering, Yosu National University, San 96-1, Dunduck-Dong, Yosu, Chonnam 550-749, South Korea*

[b] *Department of Mechanical Design Engineering, Chungnam National University, Dae-Jeon 305-764, South Korea*

Received 9 June 2003; accepted 31 October 2003

Abstract

An analytical approach is developed to investigate the vibration characteristics of the sloshing and bulging modes for a liquid-filled rigid circular cylindrical storage tank with an elastic annular plate in contact with sloshing surface of liquid. The cylindrical tank is filled with a non-viscous and incompressible liquid having a free surface. The free surface of liquid is partially covered by an annular plate with outer clamped edge and inner free edge. The liquid domain is limited by a rigid cylindrical wall and a rigid flat bottom. As the effect of free surface waves is taken into account in the analysis, the bulging and sloshing modes are studied. The solution for the velocity potential of liquid movement is assumed as a suitable harmonic function that satisfies the Laplace equation and the relevant boundary conditions. The Rayleigh–Ritz method is used to derive the frequency equation of the liquid-filled rigid cylindrical tank with an annular plate on the sloshing surface. The effects of inner-to-outer radius ratio, thickness of annular plate and liquid volume on vibration characteristics of the storage tank are studied. To demonstrate the validity of the present analytical approach, the published results are compared for the rigid cylindrical tank without a plate and the finite element analysis is performed for the tank with a plate.

1. Introduction

The motion of liquid with a free surface is of great concern in many engineering disciplines such as storage tanks or containers in airplanes, missiles, space vehicles, satellites and several others. The sloshing effect of free surface on the performance and stability of such structures is very great in the case of large scaled structures. The liquid forces and movements generated by sloshing in

*Corresponding author.
E-mail address: ywkim@yosu.ac.kr (Y.-W. Kim).

0022-460X/$ - see front matter © 2003 Elsevier Ltd. All rights reserved.
doi:10.1016/j.jsv.2003.10.032

case that the external excited frequency is close to the fundamental sloshing frequency may lead to non-controllability and destruction of the structures. The usual way to treat the troublesome problem is to alter this instability frequency. This may be achieved by covering the free surface with a flexible structure member, such as a membrane or a thin elastic plate. Immerging the annular plate (or disk)-type baffle in the liquid also is being widely used for general engineering liquid-storage tanks because it is more practical and easy to install. These make the natural sloshing frequencies deviate from the excited frequency and reduces the sloshing masses. The knowledge of the natural frequencies of the liquid or the elastic structure alone is not adequate to understand the complex liquid–structures interaction problems. The study of coupled frequencies resulting from liquid–structure interaction is very important.

There are many reports to solve the liquid–structure interaction problems of the structural elements on liquid free surface and in liquid domain. Kwak [1] and Amabili et al. [2] investigated the effect of fluid on the natural frequencies of circular plates vibrating in contact with an infinite liquid surface. Amabili and Kwak [3] investigated the effect of free-surface waves on free vibrations of circular plates resting on a free surface of infinite liquid domain. Amabili et al. [4] and Liang et al. [5] gave the natural frequencies of annular plates on an aperture of an infinite rigid wall and in contact with a fluid on one side. Bauer [6] presented the coupled hydroelastic frequencies of a liquid in a circular cylindrical rigid container, of which the free liquid surface was fully covered by a flexible membrane or an elastic circular plate. Bauer and Chiba [7] extended the study in Ref. [6] to the structure filled with incompressible viscous liquid. Amabili [8] studied the free vibrations of circular plates resting on a sloshing liquid free surface; the liquid domain was limited by a rigid cylindrical surface and a rigid flat bottom. The various kinds of devices for suppressing the dynamic motion of liquid were introduced and classified by Welt and Modi [9]. Welt and Modi [10] and Hung and Pan [11] gave the experimental results for the free vibration and dynamic response analysis of the baffled tanks. Sharma et al. [12] used a freely floating plate on the surface of fluid in order to passively control sloshing in a cylindrical container at the fundamental mode. Bauer and Komatsu [13,14] studied the coupled hydroelastic frequencies of a frictionless liquid in a circular cylindrical container, of which the free liquid surface was partially covered by an elastic annular plate. Gedikli and Erguven [15] studied the effect of an annular type baffle on the natural frequencies of liquid in a cylindrical tank using BEM, where the baffle was assumed to be rigid and immersed in liquid. Gou et al. [16] presented the non-linear dynamics of a rigid cylindrical tank with an annular baffle, where the structure was modelled on a spring–damper–mass system. Cho et al. [17] investigated vibration characteristics of an annular plate type baffled cylindrical liquid-storage tank by the coupled structural-acoustic finite element method, where the baffles were immersed in liquid. Biswal et al. [18] examined the natural frequencies of a baffled cylindrical rigid tank with an immersed annular plate using FEM.

In this paper, attention is mainly focused on the sloshing and bulging mode for a rigid circular cylindrical storage tank with an elastic annular plate on the sloshing surface. The cylindrical tank is filled with a non-viscous and incompressible liquid having a free surface. The free surface of liquid is partially covered by an elastic annular plate. The liquid domain is limited by a rigid cylindrical surface and a rigid flat bottom. Using the Rayleigh–Ritz method, the fully coupled problem between sloshing modes of the free surface and bulging modes of the annular plate is solved. To demonstrate the validity of the present analytical approach, the published results are

compared for the rigid cylindrical tank without a plate and the finite element analysis is performed for the tank with a plate.

2. Energy of the annular plate

A circular cylindrical tank of radius R (Fig. 1) is filled to a height H with an incompressible and non-viscous liquid of density ρ_L. The cylindrical wall at $r = R$ and the tank bottom at $x = 0$ are considered as rigid walls, while the free surface at $x = H$ is partially covered with an elastic annular plate of uniform thickness h_p, density ρ_p and inner radius a. The polar co-ordinate system (r, θ) for the plate is introduced at the center of the annular plate. The considered annular plate, which is vibrating in vacuum, is assumed to be made of linearly elastic, homogeneous and isotropic material. Moreover, the effect of shear deformation and rotary inertia is neglected. The equation of motion for transverse displacement, w, of annular plate is

$$D\left(\frac{\partial^2}{\partial r^2}+\frac{1}{r}\frac{\partial}{\partial r}+\frac{1}{r^2}\frac{\partial^2}{\partial\theta^2}\right)^2 w+\rho_P h_P\frac{\partial^2 w}{\partial t^2}=0, \tag{1}$$

where $D = Eh_p^3/12(1-\nu^2)$ is the flexible rigidity of the plate; ν and E are the Poisson ratio and elastic modulus.

The classical methods of finding the solutions of this equation are based on the separation of variables. In the case of axisymmetric boundary conditions the solution in vacuum takes the form [4,5]

$$w(r,\theta,t)=\cos n\theta\sum_{m=0}^{\infty}W_{nm}(r)q_m e^{i\omega t}, \tag{2}$$

where

$$W_{nm}(r)=A_{nm}\left[J_n\left(\frac{\lambda_{nm}r}{R}\right)+B_{nm}I_n\left(\frac{\lambda_{nm}r}{R}\right)+C_{nm}Y_n\left(\frac{\lambda_{nm}r}{R}\right)+D_{nm}K_n\left(\frac{\lambda_{nm}r}{R}\right)\right], \tag{3}$$

in which $A_{nm}, B_{nm}, C_{nm}, D_{nm}$ are mode shape constants that are determined by the boundary conditions. q_m are the Ritz unknown coefficients, n is the number of nodal diameters, m is the number of nodal circles. J_n and Y_n are the Bessel functions of the first and second kinds, I_n and K_n

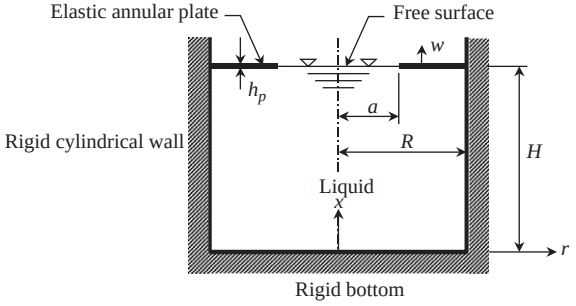

Fig. 1. Considered cylindrical storage tank with an elastic annular plate on liquid surface.

are the modified Bessel functions of the first and second kinds, and λ_{nm} is the frequency parameter which is determined by the boundary condition. The annular plate may be attached to the cylindrical wall with various boundary conditions such as clamped, simply supported, free, guided or elastically supported boundary condition. In this paper, however, it is considered only that the annular plate is clamped at $r = R$ and free at $r = a$. The frequency parameter λ_{nm} is related to the circular frequency ω_{nm} of the plate in vacuum:

$$\omega_{nm} = \frac{\lambda_{nm}^2}{R^2}\sqrt{\frac{D}{\rho_p h_p}}. \tag{4}$$

The mode shapes for free vibrations of thin elastic plates coupled to the liquid are expanded by using the solution in vacuum as the admissible function [1–5,8].

To simplify the computations, the mode shape constants are normalized so that

$$\int_a^R W_{nm}^2(r) r \, \mathrm{d}r = 1. \tag{5}$$

From Eq. (5), the mode shape constant A_{nm} is

$$A_{nm} = \left[\int_a^R \left\{ \mathrm{J}_n\left(\frac{\lambda_{nm} r}{R}\right) + B_{nm}\mathrm{I}_n\left(\frac{\lambda_{nm} r}{R}\right) + C_{nm}\mathrm{Y}_n\left(\frac{\lambda_{nm} r}{R}\right) + D_{nm}\mathrm{K}_n\left(\frac{\lambda_{nm} r}{R}\right)\right\}^2 r \, \mathrm{d}r\right]^{-1}. \tag{6}$$

In order to solve the problem, the kinetic and potential energies of the plate are evaluated. The reference kinetic energy T_p of the plate is given by

$$T_p = \tfrac{1}{2}\rho_p h_p \int_0^{2\pi}\int_a^R w^2(r,\theta) r \, \mathrm{d}r = \tfrac{1}{2}\psi_n \rho_p h_p \sum_{m=0}^{\infty} q_m^2, \tag{7}$$

where $\psi_n = \pi$ for $n > 0$ and $\psi_n = 2\pi$ for $n = 0$.

The maximum potential energy of the plate in vacuum is equal to the reference kinetic energy of the same mode multiplied by the circular frequency ω_{nm}^2 of this mode

$$U_p = \omega_{nm}^2 T_p = \tfrac{1}{2}\psi_n \frac{D}{R^4}\sum_{m=0}^{\infty}\lambda_{nm}^4 q_m^2. \tag{8}$$

3. Energy of liquid

A cylindrical co-ordinate system (x, r, θ) for the liquid domain is introduced as shown in Fig. 1. The tank is filled with a non-viscous and incompressible liquid, with a free surface orthogonal to the vertical tank axis. The surface tension of the liquid and the hydrostatic pressure effect are neglected in the present study.

For an incompressible and non-viscous liquid, the deformation potential must satisfy the following Laplace equation [3–5,8,14,15]:

$$\left(\frac{\partial^2}{\partial x^2} + \frac{\partial^2}{\partial r^2} + \frac{1}{r}\frac{\partial}{\partial r} + \frac{1}{r^2}\frac{\partial^2}{\partial \theta^2}\right)\phi = 0. \tag{9}$$

The boundary conditions imposed to the liquid are: (a) contact at the liquid–rigid bottom interface; (b) contact at the liquid–rigid lateral cylindrical interface; (c) contact at the liquid–plate interface for $a \leqslant r \leqslant R$; and (d) the linearized sloshing condition at the free surface of the liquid for $0 \leqslant r \leqslant a$. Therefore,

$$\left.\frac{\partial \phi}{\partial x}\right|_{x=0} = 0, \tag{10}$$

$$\left.\frac{\partial \phi}{\partial r}\right|_{r=R} = 0, \tag{11}$$

$$\left.\frac{\partial \phi}{\partial x}\right|_{x=H} = \begin{cases} \dfrac{\omega^2}{g}\,\phi|_{x=H} & \text{for } 0 \leqslant r \leqslant a, \\ w & \text{for } a \leqslant r \leqslant R, \end{cases} \tag{12a, b}$$

where g is the gravity acceleration and ω is the circular frequency of vibration of the coupled system. If the plate is not considered, the free surface range of $0 \leqslant r \leqslant a$ in Eq. (12a) is replaced to $0 \leqslant r \leqslant R$.

The deformation potential satisfying Eq. (9), by using the separation of variables with respect to considered co-ordinate, is assumed to be of the form for the asymmetric mode ($n > 0$):

$$\phi(x, r, \theta) = \cos n\theta \sum_{k=0}^{\infty} p_{nk} \mathrm{J}_n\left(\frac{\varepsilon_{nk} r}{R}\right) \frac{\cosh(\varepsilon_{nk} x/R)}{\cosh(\varepsilon_{nk} H/R)}, \tag{13}$$

where k and n are the numbers of nodal circles and diameters of free surface wave.

Eq. (13) satisfies the boundary condition (10) but does not condition (11) yet. The following equation is obtained by applying this assumed deformation potential into Eq. (11):

$$\frac{\mathrm{d}\mathrm{J}_n(\varepsilon_{nk})}{\mathrm{d}r} = 0. \tag{14}$$

Eq. (13) satisfies the boundary condition (11) by using the roots of Eq. (14). Eq. (13) is not adaptable to the axisymmetric mode ($n = 0$) because the first root is zero $\varepsilon_{00} = 0$. This deformation potential must be modified to express the axisymmetric mode. The axisymmetric mode of $(n, k) = (0, 0)$ only occurs in rigid motion when the plate vibrates in this mode because the considered liquid is incompressible. Therefore, for the axisymmetric mode including this $(n, k) = (0, 0)$ mode, the deformation potential is changed to

$$\phi(x, r, \theta) = p_{00} + \sum_{k=1}^{\infty} p_{0k} \mathrm{J}_0\left(\frac{\varepsilon_{0k} r}{R}\right) \frac{\cosh(\varepsilon_{0k} x/R)}{\cosh(\varepsilon_{0k} H/R)}. \tag{15}$$

The reference kinetic energy of liquid due to liquid–plate interaction is expressed as

$$T_L = \tfrac{1}{2}\rho_L \int_0^{2\pi} \int_a^R \phi|_{x=H} \left.\frac{\partial \phi}{\partial x}\right|_{x=H} r\,\mathrm{d}r = \tfrac{1}{2}\rho_L \int_0^{2\pi} \int_a^R \phi|_{x=H} w(r, \theta) r\,\mathrm{d}r. \tag{16}$$

From Eq. (16), for the asymmetric mode ($n > 0$), the reference kinetic energy of liquid is given by

$$T_L = \tfrac{1}{2}\rho_L \psi_n \sum_{m=0}^{\infty}\sum_{k=0}^{\infty} \beta_{nmk} p_{nk} q_m. \tag{17}$$

For the axisymmetric mode ($n = 0$), Eq. (17) is replaced by

$$T_L = \tfrac{1}{2}\rho_L \psi_0 \sum_{m=0}^{\infty}\left[\gamma_{0m} p_{00} + \sum_{k=1}^{\infty} \beta_{0mk} p_{0k}\right] q_m. \tag{18}$$

4. Sloshing equation of liquid

To obtain the sloshing equation of liquid, one should apply the deformation potentials into the free surface condition (12a) and the compatibility condition (12b). By using Eq. (13), for the asymmetric mode ($n > 0$), one has

$$\sum_{k=1}^{\infty} p_{nk} \frac{\varepsilon_{nk}}{R} \mathrm{J}_n\left(\frac{\varepsilon_{nk} r}{R}\right) \tanh\left(\frac{\varepsilon_{nk} H}{R}\right) = \left[\frac{\omega^2}{g} \sum_{k=0}^{\infty} p_{nk}\, \mathrm{J}_n\left(\frac{\varepsilon_{nk} r}{R}\right)\right]_{0 \leqslant r \leqslant a} + \left[\sum_{m=0}^{\infty} W_{nm}(r) q_m\right]_{a \leqslant r \leqslant R}. \tag{19}$$

Eq. (19) must be satisfied for all $0 \leqslant r \leqslant R$. Therefore, multiplying Eq. (19) by $\mathrm{J}_n(\varepsilon_{nj} r/R) r$ and integrating between 0 and R, one obtains the following sloshing equation:

$$\sum_{k=0}^{\infty}\sum_{j=0}^{\infty} \frac{\varepsilon_{nk}}{R} \tanh\left(\frac{\varepsilon_{nk} H}{R}\right) \alpha_{nkj} p_{nk} - \sum_{m=0}^{\infty}\sum_{j=0}^{\infty} \beta_{nmj} q_m = \frac{\omega^2}{g} \sum_{k=0}^{\infty}\sum_{j=0}^{\infty} \bar{\alpha}_{nkj} p_{nk}, \tag{20}$$

where α_{nkj}, $\bar{\alpha}_{nkj}$ and β_{nmj} are given in Appendix A.

For the axisymmetric mode ($n = 0$), the following equation by using Eq. (15) is added in Eq. (19):

$$0 = \frac{\omega^2}{g}\left[p_{00} + \sum_{k=1}^{\infty} p_{0k} \mathrm{J}_0\left(\frac{\varepsilon_{0k} r}{R}\right)\right]_{0 \leqslant r \leqslant a} + \left[\sum_{m=0}^{\infty} W_{0m}(r) q_m\right]_{a \leqslant r \leqslant R}. \tag{21}$$

Multiplying this equation by $r\,\mathrm{d}r$ and integrating between 0 and R, one obtains

$$-\sum_{m=0}^{\infty} \gamma_{0m} q_m = \frac{\omega^2}{g}\left[\frac{a^2}{2} p_{00} + \sum_{k=1}^{\infty} p_{0k} \eta_{0k}\right], \tag{22}$$

where γ_{0m} and η_{0k} are given in Appendix A.

Therefore, the sloshing equation for the axisymmetric mode is modified to

$$\begin{aligned}\sum_{k=1}^{\infty}\sum_{j=1}^{\infty} \frac{\varepsilon_{0k}}{R} \tanh\left(\frac{\varepsilon_{0k} H}{R}\right) \alpha_{0kj} p_{0k} - \sum_{m=0}^{\infty}\left[\gamma_{0m} + \sum_{j=1}^{\infty} \beta_{0mj}\right] q_m \\ = \frac{\omega^2}{g}\left[\frac{a^2}{2} p_{00} + \sum_{k=1}^{\infty} \eta_{0k} p_{0k} + \sum_{j=1}^{\infty} \eta_{0j} p_{0j} + \sum_{k=1}^{\infty}\sum_{j=1}^{\infty} \bar{\alpha}_{0kj} p_{0k}\right].\end{aligned} \tag{23}$$

5. Eigenvalue problem

For the numerical calculation of the natural frequencies and the parameters of Ritz expansion of modes, M terms in the expansion of w of Eq. (2) and K in the expansion of ϕ of Eqs. (13) and (15) are selected.

In Rayleigh–Ritz method, it is useful to introduce Rayleigh's quotient in order to obtain the vibration characteristics:

$$\omega^2 = \frac{U_p}{T_p + T_L}. \tag{24}$$

The reference kinetic and the maximum potential energy of the plate from Eqs. (7) and (8) can be expressed in matrix forms of

$$T_p = \tfrac{1}{2}\psi_n q^{\mathrm{T}}[M_p]q, \tag{25}$$

$$U_p = \tfrac{1}{2}\psi_n q^{\mathrm{T}}[K_p]q, \tag{26}$$

where $q^{\mathrm{T}} = \{\, q_0 \quad q_1 \quad \dots \quad q_M \,\}$. The stiffness and mass matrices of the plate, $[M_p]$ and $[K_p]$, are

$$[K_p]_{mi} = \delta_{mi}\frac{D}{R^4}\lambda_{ni}^4, \quad [M_p]_{mi} = \rho_p h_p \delta_{mi}, \tag{27}$$

where δ_{mi} is the Kronecker delta and $m, i = 0, \dots, M$.

The reference kinetic energy of liquid, Eqs. (17) or (18), may be written as

$$T_L = \tfrac{1}{2}\psi_n q^{\mathrm{T}}[M_L]p, \tag{28}$$

where $p^{\mathrm{T}} = \{\, p_0 \quad p_1 \quad \dots \quad p_K \,\}$ and $[M_L]$ is the coupled force matrix describing the inertial effect of the liquid inside the tank.

The elements of the matrix $[M_L]$ of dimension $(M+1)\times(K+1)$ for the asymmetric $(n>0)$ are given by

$$[M_L]_{mk} = \rho_L \beta_{nmk}, \quad m = 0, 1, \dots, M \ \text{ and } \ k = 0, 1, \dots, K. \tag{29}$$

And for the asymmetric mode $(n=0)$, the elements of the matrix $[M_L]$ are

$$[M_L] = [\,[M_L]_{m0} \quad [M_L]_{mk}\,], \quad m = 0, 1, \dots, M \ \text{ and } \ k = 1, \dots, K, \tag{30}$$

where

$$[M_L]_{m0} = \rho_L \gamma_{m0}, \quad [M_L]_{mk} = \rho_L \beta_{0mk}. \tag{31a, b}$$

Minimizing Rayleigh's quotient, one obtains the following equation:

$$[K_p]q - \omega^2\big[[M_p]q + [M_L]p\big] = 0. \tag{32}$$

The sloshing Eqs. (20) and (23) can be rewritten in the matrix form:

$$[K_{ps}]q + [K_s]p - \omega^2[M_s]p = 0, \tag{33}$$

where the elements of matrices $[K_{ps}]$ of dimension $(K+1)\times(M+1)$, $[K_s]$ and $[M_s]$ of dimension $(K+1)\times(K+1)$ in Eq. (33) for the asymmetric mode $(n>0)$ are

$$[K_{ps}]_{km} = -\beta_{nmk}, \tag{34}$$

$$[K_s]_{kj} = \delta_{kj}\frac{\varepsilon_{nk}}{R}\tanh\left(\frac{\varepsilon_{nk}H}{R}\right)\alpha_{nkj}, \tag{35}$$

$$[M_s]_{kj} = \frac{\bar{\alpha}_{nkj}}{g}, \tag{36}$$

in which $m = 0, 1, \ldots, M,$ and $k(\text{or } j) = 0, 1, \ldots, K.$

For the axisymmetric mode ($n = 0$) the elements of matrices $[K_{ps}]$, $[K_s]$ and $[M_s]$ in Eq. (33) are modified by

$$[K_{ps}] = \lfloor\, [K_{ps}]_{0k} \quad [K_{ps}]_{km} \,\rfloor, \quad [K_{ps}]_{0k} = -\gamma_{0k}, \quad [K_{ps}]_{km} = -\beta_{0mk}, \tag{37}$$

$$[K_s] = \begin{bmatrix} 0 & 0 \\ 0 & [K_s]_{kj} \end{bmatrix}, \quad [K_s]_{kj} = \delta_{kj}\frac{\varepsilon_{0k}}{R}\tanh\left(\frac{\varepsilon_{0k}H}{R}\right)\alpha_{0kj}, \tag{38}$$

$$[M_s] = \begin{bmatrix} M_{s00} & [M_s]_{0j} \\ [M_s]_{k0} & [M_s]_{kj} \end{bmatrix}, \quad M_{s00} = \frac{a^2}{2g},$$

$$[M_s]_{0j} = \frac{\eta_{0j}}{g}, \quad [M_s]_{k0} = \frac{\eta_{0k}}{g}, \quad [M_s]_{kj} = \frac{\bar{\alpha}_{0kj}}{g}. \tag{39}$$

The stiffness and mass matrices of liquid, $[K_s]$ and $[M_s]$, have contribution only from the free surface of liquid. $[K_{ps}]$ is also the coupled force matrix with $\rho_L[K_{ps}] = -[M_L]^{\mathrm{T}}$ relationship.

The eigenvalue problem takes the following final form by adding the sloshing Eq. (33) to eigenvalue problem (32):

$$\begin{bmatrix} [K_p] & [0] \\ [K_{ps}] & [K_s] \end{bmatrix}\begin{Bmatrix} q \\ p \end{Bmatrix} - \omega^2\begin{bmatrix} [M_p] & [M_L] \\ [0] & [M_s] \end{bmatrix}\begin{Bmatrix} q \\ p \end{Bmatrix} = 0. \tag{40}$$

This equation is a linear eigenvalue problem for a real, non-symmetric matrix, thus extraction of eigenvalues and the corresponding eigenvectors becomes difficult particularly when very large size matrices are involved. The eigenvalue problem can be transformed into one for symmetric matrix using $\rho_L[K_{ps}] = -[M_L]^{\mathrm{T}}$. Thus,

$$\begin{bmatrix} [K_p] + [M_L][\bar{M}_s]^{-1}[M_L]^{\mathrm{T}} & -[M_L][\bar{M}_s]^{-1}[\bar{K}_s] \\ -[\bar{K}_s][\bar{M}_s]^{-1}[M_L]^{\mathrm{T}} & [\bar{K}_s][\bar{M}_s]^{-1}[\bar{K}_s] \end{bmatrix}\begin{Bmatrix} q \\ p \end{Bmatrix} - \omega^2\begin{bmatrix} [M_p] & 0 \\ 0 & [\bar{K}_s] \end{bmatrix}\begin{Bmatrix} q \\ p \end{Bmatrix} = 0, \tag{41}$$

where

$$[\bar{K}_s] = \rho_L[K_s], \quad [\bar{M}_s] = \rho_L[M_s]. \tag{42}$$

Consequently, the determination of natural frequencies and the corresponding mode shapes from Eq. (41) is much simpler than from Eq. (40).

As being extended the free surface region from $0 \leqslant r \leqslant a$ to $0 \leqslant r \leqslant R$ for the first term of right side of Eq. (19), the sloshing frequency equation of the rigid cylindrical shell without annular plate cover is derived as follows:

$$\omega^2 = g\frac{\varepsilon_{nk}}{R}\tanh\left(\frac{\varepsilon_{nk}H}{R}\right). \tag{43}$$

This equation can be found in Ref. [6,14].

6. Numerical results and discussion

To check the validity of the present analytical approach, some comparisons are made with the published data and the finite element analysis results. ANSYS commercial FEM code [19] is used for the finite element analysis procedures. In the finite element analysis, a two-dimensional axisymmetric model is constructed with the axisymmetric structural shell element for the elastic structures and fluid element for the liquid region. The shell element has two nodes and four degrees of freedom at each node: three translations in the each nodal direction and a rotation. The fluid element is defined by four nodes having three degrees of freedom at each node: three translations in the each nodal direction. The radial displacements of liquid nodes along the rigid cylindrical wall to present Eq. (10) are constrained. The liquid boundary conditions at the bottom of the tank are zero axial displacement to simulate Eq. (11). The axial displacements of liquid nodes along the wetted plate surfaces coincide with the corresponding displacements of the plate to simulate Eq. (12b). The eigenvalue problem formulated within the FEM for the vibration analysis is solved by the reduced subspace analysis method to consider the free surface of liquid.

The material properties of the annular plate and liquid are: $E = 72\,\text{GPa}$, $v = 0.3$, $\rho_p = 2780\,\text{kg/m}^3$, and $\rho_L = 1000\,\text{kg/m}^3$. To verify the present methodology, the sloshing frequencies of liquid expressed as non-dimensional parameters ($\Omega_n = \omega_n\sqrt{R/g}$) in the rigid cylindrical tank without plate are compared with existing results [15,18] for the $n = 1$ modes as shown in Fig. 2. It is observed that the computed results are quite comparable with the existing results. Also the present FEA results are compared with the present analytical results for the cylindrical storage tank with $R = 1\,\text{m}$, $a/R = 0.7$, $h_p = 4\,\text{mm}$ and $H = 0.2R$ in Table 1. The agreement between the results is very good and the discrepancy is less than 2.1% for sloshing modes, and 6.0% for bulging modes. The discrepancy in the table is calculated by $(f_A - f_F)/f_A \times 100$, where, f_A is the frequency from the analytical approach and f_F is that from FEA. The frequencies from the analytical approach are somewhat higher than those from the finite element method. This is the reason that the analytical results generally provide the upper bounds. The fundamental sloshing frequency occurs in $(n, k) = (1, 0)$ mode because the considered liquid is incompressible. The mode of $(n, k) = (1, 0)$ in the sloshing mode shape does not occur because there is no plate rigid motion for $n = 0$ mode.

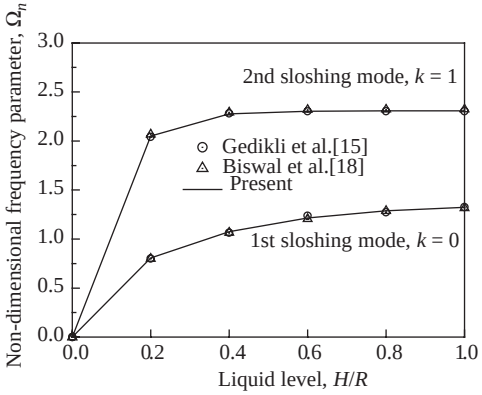

Fig. 2. Variation of the sloshing frequencies for $n = 1$ mode with various liquid levels of rigid cylindrical tank without plate.

Table 1
Comparison of the sloshing and bulging frequencies for the first 10 modes with FEM results ($R = 1\,\text{m}$, $a = 0.7\,\text{m}$, $h = 4\,\text{mm}$, $H/L = 0.2$)

Sloshing mode				Bulging mode			
Modes (n, k)	Analytical approach	FEM	Disc. (%)	Modes (n, m)	Analytical approach	FEM	Disc. (%)
1 (1,0)	0.6262	0.6291	−0.4631	1 (0,0)	11.014	10.591	3.8406
2 (2,0)	1.0011	0.9938	0.7292	2 (1,0)	11.518	11.231	2.4918
3 (0,1)	1.0477	1.0554	−0.7349	3 (2,0)	13.993	13.688	2.1797
4 (3,0)	1.2713	1.2567	1.1484	4 (3,0)	17.970	17.248	4.0178
5 (1,1)	1.3341	1.3071	2.0238	5 (4,0)	23.008	22.104	3.9291
6 (4,0)	1.4730	1.4535	1.3238	6 (5,0)	29.558	28.114	4.8853
7 (2,1)	1.5524	1.5196	2.1129	7 (6,0)	37.236	35.331	5.1160
8 (0,2)	1.5651	1.5741	−0.5750	8 (7,0)	46.465	43.887	5.5483
9 (5,0)	1.6335	1.6133	1.2366	9 (8,0)	57.285	53.932	5.8532
10 (3,1)	1.7260	1.6928	1.9235	10 (9,0)	69.604	65.593	5.7626

(n, k) and (n, m): n and k (or m) denote the number of nodal diameters and nodal circles.
Disc.: discrepancy.

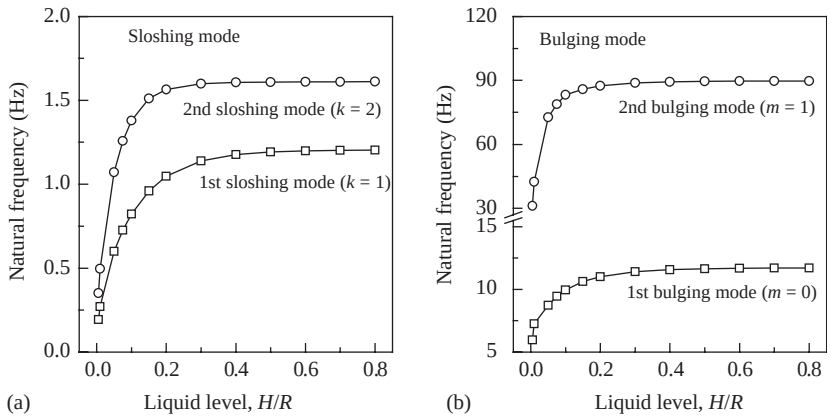

Fig. 3. Variation of the sloshing and bulging frequencies for $n = 0$ mode with various liquid levels ($R = 1\,\text{m}$, $h_p = 4\,\text{mm}$, $a/R = 0.7$).

Fig. 3 shows the frequency variation of the axisymmetric mode of $n = 0$ with various liquid levels for the storage tank used in Table 1. The frequencies first increase to any converged values and then remain constant with the increase of liquid level. This means that there is no effect of liquid level in case that the liquid is filled to above half of the radius of storage tanks. The mode of $k = 0$ does not occur because there is no plate rigid motion in the sloshing mode shape for $n = 0$ mode as stated in Table 1. Fig. 4 indicates the frequency variation of the asymmetric mode of $n = 2$ with various liquid levels for the storage tank used in Fig. 3. The general behavior is similar to the axisymmetric mode as shown in Fig. 3. As presented in Figs. 3 and 4, the effect of liquid level becomes great as the number of nodal circles k or m increases in the small liquid level, that is,

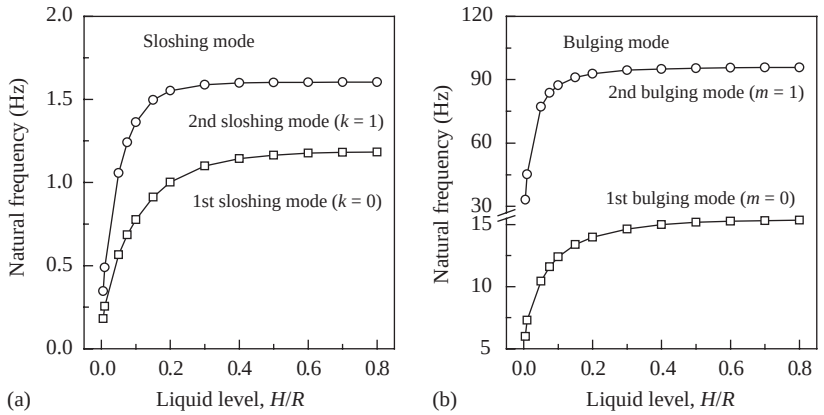

Fig. 4. Variation of the sloshing and bulging frequencies for $n = 2$ mode with various liquid levels ($R = 1$ m, $h_p = 4$ mm, $a/R = 0.7$).

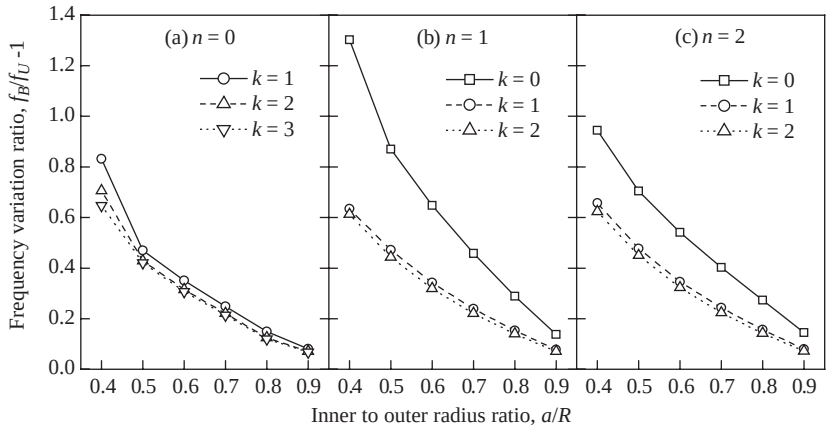

Fig. 5. Effect of inner-to-outer radius ratio of annular plates on the sloshing frequencies ($R = 1$ m, $h_p = 4$ mm, $H/R = 0.5$).

the frequencies become constant more rapidly with increase of the number of nodal circles. To check the effect of liquid level on natural frequencies of the considered storage tank, one may consider the liquid level only up to half of the radius of the tank.

Fig. 5 presents the effect of inner-to-outer radius ratio of annular plate on the first three sloshing frequencies for each $n = 0$, 1 and 2. The storage tank with an annular plate of $h_p = 4$ mm is filled up to $H = 0.5R$ ($R = 1$ m) with liquid. The frequency variation ratio used in the figure is calculated from f_B/f_U–1, where f_B is the sloshing frequency for the tank with a plate and f_U is for the tank without a plate. As shown in this figure, the sloshing frequencies decrease non-linearly with increase of this ratio or increase of the free surface. The effect of a/R ratio in lower modes is much larger than in higher modes. That is, this effect decreases as the number of nodal circle k increases. This effect is the largest for the $n = 1$ mode and the least for the $n = 0$ mode. This means this effect in lower modes is greater than in higher modes also. For example, the frequency

of $(n, k) = (1, 0)$ mode increases about 130% and that of $(n, k) = (1, 1)$ mode does about 60% by attaching the annular plate of $a/R = 0.4$ compared with the sloshing frequency of the tank without a plate.

Fig. 6 gives the effect of inner-to-outer radius ratio of annular plate on the first three bulging frequencies for each $n = 0$, 1 and 2 for the tank used in Fig. 5. The frequency variation ratio used in the figure is defined by $f_C/f_V - 1$, where f_C is the bulging frequency of the annular plate coupled with liquid and f_V is that of the plates in vacuum. The negative value of this frequency ratio means the reduction of frequency by liquid coupling. The bulging frequencies decrease much more by liquid coupling except for some modes as this radius ratio becomes small. For example, the frequency in $(n, m) = (2, 0)$ mode decreases about 60% for $a/R = 0.9$ and about 75% for $a/R = 0.4$. The effect of a/R ratio in lower modes is much larger than in higher modes. For small a/R ratio < 0.6, the frequencies of $m = 0$ mode for $n = 0$ and 1 decrease very large, above 85%, compared with other modes because the bulging modes occur simultaneously with the first sloshing modes. The frequency reduction, however, becomes small as the radius ratio is below 0.5 for these modes. The reason for this behavior is that the sloshing frequency and bulging frequency have the same value with the result that the first bulging modes occur simultaneously with the first sloshing modes. The free surface decreases as this ratio increases in the case of $a/R < 0.5$. In result, the bulging frequency decreases less by the liquid coupling because the sloshing (or bulging) frequency increases as this ratio increases.

The first three bulging mode shapes with a/R ratios of $n = 1$ mode present in Fig. 7. As shown in this figure, $m = 0$ mode shape of the plate with $a/R = 0.5$ is equal to sloshing mode shape, that is, the bulging modes occur simultaneously with the first sloshing modes. The reason for this is that the liquid coupling effect is very large as the contact surface of plate with liquid become large. The relative amplitude of the plate is very small compared with that of the free surface in this mode. The free surface motion declines and the bulging motion becomes dominant as the a/R ratio increases. The free surface motion becomes small as the number of nodal circle m increases.

Fig. 8 demonstrates the effect of the annular plate's thickness on the sloshing and bulging frequency variation for the tank with an annular plate of $a/R = 0.7$, $R = 1\,\text{m}$, $H = 0.25R$. The

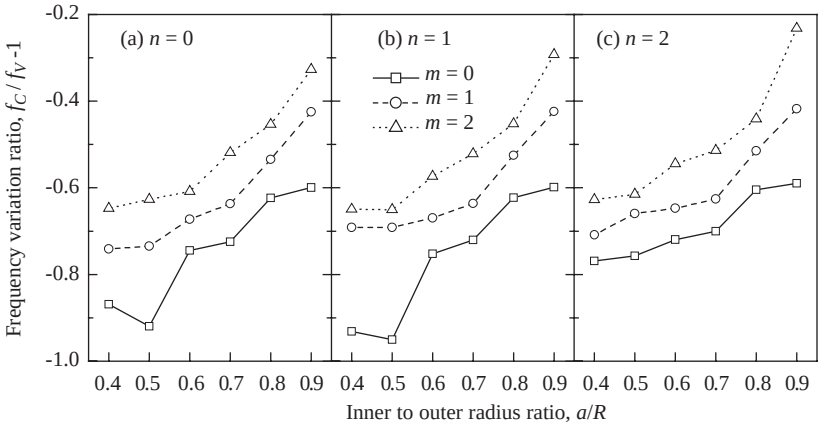

Fig. 6. Effect of inner-to-outer radius ratio of annular plates on the bulging frequencies ($R = 1\,\text{m}$, $h_p = 4\,\text{mm}$, $H/R = 0.5$).

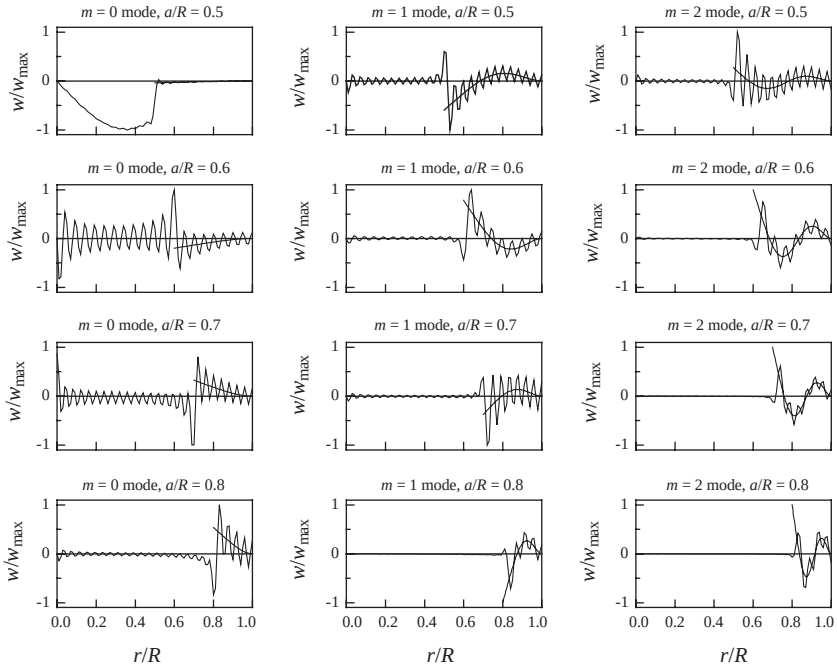

Fig. 7. Effect of inner-to-outer radius ratio on the first three bulging mode shapes for $n = 1$ mode ($h_p = 4$ mm, $R = 1$ m, $H = 0.5$ m).

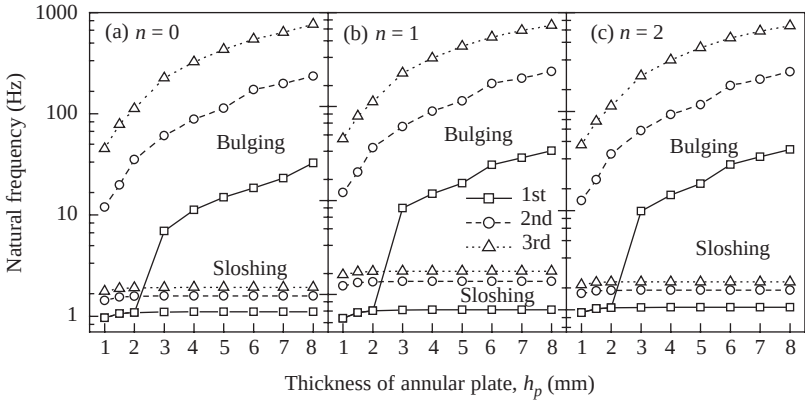

Fig. 8. Effect of plate thickness on the sloshing and bulging frequencies ($R = 1$ m, $a/R = 0.7$, $H/R = 0.25$).

sloshing frequency is very small compared with the bulging frequency. In the case of very thin plate, the first sloshing and bulging frequencies are same. This means that these two modes occur simultaneously because the liquid coupling effect is very large. The bulging and sloshing modes are separated as the thickness of plate becomes above 2 mm. The sloshing frequency first increases in small thickness and then remains constant as the thickness becomes thick. The reason for this is that the free surface always remains constant because there is no deformation of the plate in sloshing mode shapes in the case of the tank with the relatively thick plate. Therefore, the sloshing

frequency does not vary because the kinetic energy of liquid due to the free surface motion is constant. For the tanks with very thin plates, however, the sloshing frequency varies with the thickness of plate because the deformation of the plate occurs simultaneously with free surface motion. The bulging frequency increases as the thickness becomes thick. The reason for this is that the rigidity of plate increases as the thickness becomes thick.

Figs. 9–11 illustrate the sloshing and bulging mode shape variations with thickness of the annular plate for the tank used in Fig. 8. The mode shapes of a tank with an annular plate of $h_p = 1$ mm are presented in Fig. 9. The plate is deformed simultaneously by liquid coupling as the sloshing mode shapes. For the second sloshing mode shapes, the relative deformation of the plate is small compared with that of the free surface of liquid. The first bulging mode shape is the same as the first sloshing mode shape. In the second bulging mode shapes, the deformation of the plate is large compared with that of liquid. The mode shapes of $n = 0$ mode for the tank with an annular plate of $h_p = 2$ mm as given in Fig. 10 are very similar to Fig. 9. For $n = 1$ sloshing mode shapes, however, the relative deformation of the plate is small since the effect of liquid coupling on plate deformation is not large due to high rigidity of the plate. From this, one can estimate that there will be no deformation of plate in sloshing mode shapes in case that the thickness becomes large. Fig. 11 shows the mode shapes for the tank with an annular plate of $h_p = 4$ mm. There is no deformation of plate in sloshing mode shapes as expected in Fig. 10. The first bulging mode is separated from the sloshing mode unlike the tank with a thin plate. In the second bulging mode, the deformation of liquid is small compared with that of plate. This means

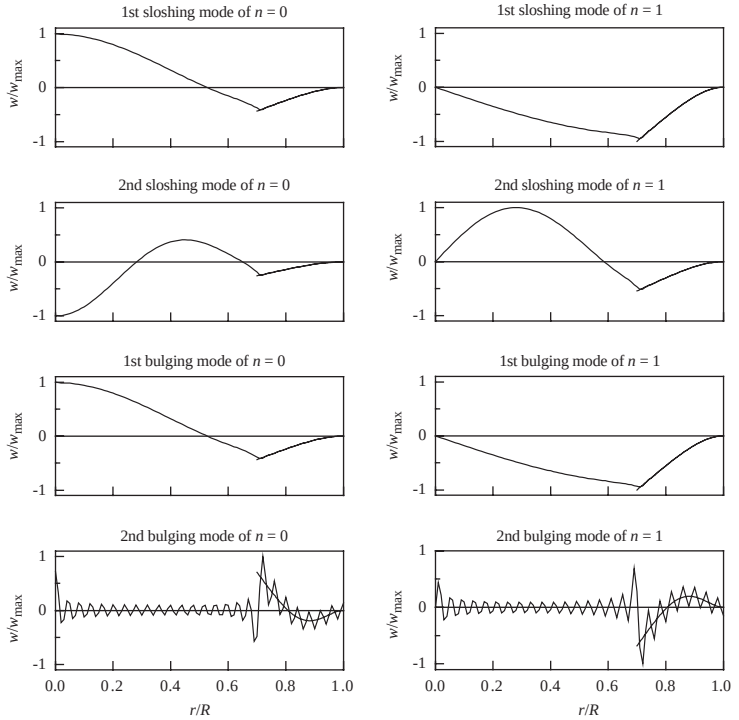

Fig. 9. Mode shapes of the first two sloshing and bulging modes for $n = 0$ and 1 modes ($h_p = 1$ mm, $a/R = 0.7$, $R = 1$ m, $H = 0.25$ m).

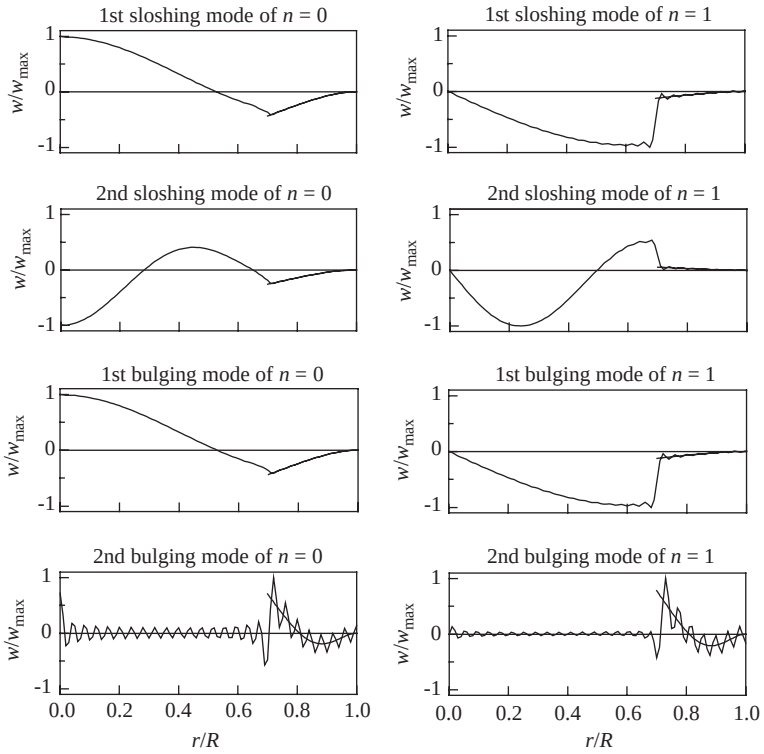

Fig. 10. Mode shapes of the first two sloshing and bulging modes with $n = 0$ and 1 mode ($h_p = 2\,\text{mm}$, $a/R = 0.7$, $R = 1\,\text{m}$, $H = 0.25\,\text{m}$).

that the sloshing mode shapes are characterized by only liquid motion and the bulging mode shapes by only plate motion as the plate becomes thick. As shown in Figs. 9 and 10, the reason why $k = 0$ mode does not occur in sloshing mode shapes although the plate is deformed is that $k = 0$ mode shape is modified to $k = 1$ mode shape by the plate deformation.

7. Conclusions

An analytical approach is used to investigate the vibration characteristics of the sloshing and bulging mode for a circular cylindrical storage tank with an annular plate on sloshing surface. The cylindrical tank is filled with a non-viscous and incompressible liquid having a free surface. The free surface of liquid is partially covered by an elastic annular plate. The liquid domain is limited by a rigid cylindrical wall and a rigid flat bottom. To demonstrate the validity of the present analytical approach, the published results are compared for the rigid cylindrical tank without a plate and the finite element analysis is performed for the tank with a plate. Based on the numerical results, the followings are concluded.

The effect of liquid level on the sloshing and bulging frequency is great, but this effect is constant in the case of the liquid being filled to above half of the radius of the storage tank. By attaching the annular plate on the free surface, the sloshing frequencies of liquid increase due to

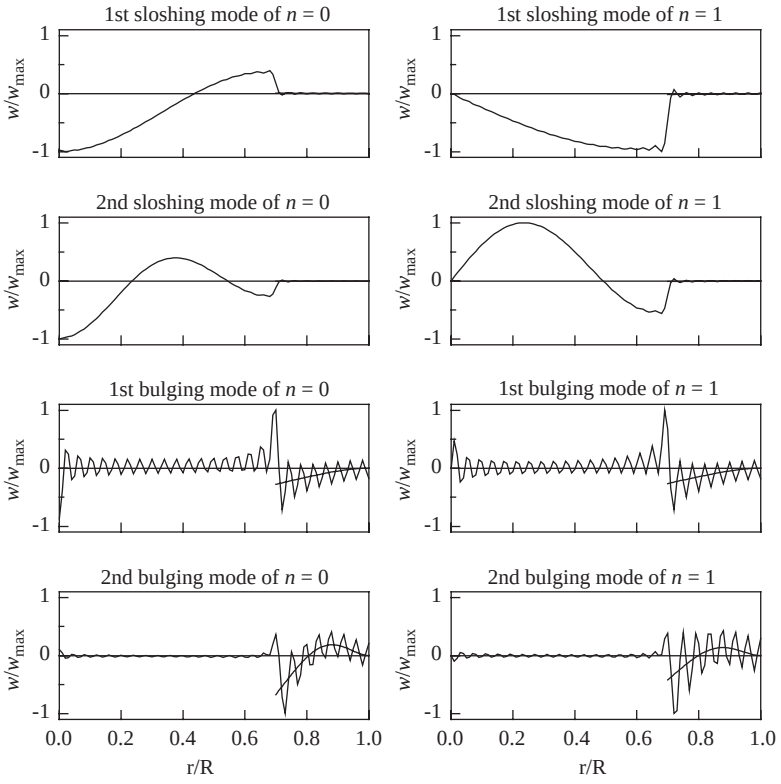

Fig. 11. Mode shapes of the first two sloshing and bulging modes with $n = 0$ and 1 mode ($h_p = 4\,\text{mm}$, $a/R = 0.7$, $R = 1\,\text{m}$, $H = 0.25\,\text{m}$).

decrease of the free surface and the bulging frequencies of plate decrease due to liquid coupling effect. The coupling effect on the bulging modes become great as the inner to outer radius ratio becomes small. The effect of this radius ratio on the natural frequency is greater in lower modes than in higher modes. The sloshing and bulging frequency increases with the increase of plate thickness. Above any thickness the sloshing frequency remains constant. The sloshing and bulging modes occur simultaneously of are coupled if the plate has very thin thickness or small a/R ratio. Conversely, the sloshing mode shapes are characterized by only the liquid motion and the bulging mode shapes by only the plate motion as the thickness of the plate becomes thick or the inner radius does large.

Appendix A

The coefficients α_{nkj}, $\bar{\alpha}_{nkj}$ and β_{nmj} in Eq. (21) are as follows:

$$\alpha_{nkj} = \int_0^R \mathrm{J}_n\left(\frac{\varepsilon_{nk} r}{R}\right)\mathrm{J}_n\left(\frac{\varepsilon_{nj} r}{R}\right) r\,\mathrm{d}r = \frac{R^2}{2}\left[1 - \frac{n^2}{\varepsilon_{nk}^2}\mathrm{J}_n^2(\varepsilon_{nk})\right]\delta_{kj}, \tag{A.1}$$

where δ_{kj} is the Kronecker delta.

$$\bar{\alpha}_{nkj} = \int_0^a \mathrm{J}_n\left(\frac{\varepsilon_{nk}r}{R}\right)\mathrm{J}_n\left(\frac{\varepsilon_{nj}r}{R}\right)r\,\mathrm{d}r = \begin{cases} \dfrac{a^2}{2}\left[\mathrm{J}'_n 2\left(\dfrac{\varepsilon_{nk}a}{R}\right) + \left(1 - \dfrac{n^2}{\varepsilon_{nk}^2 a^2/R^2}\right)\mathrm{J}_n^2\left(\dfrac{\varepsilon_{nk}a}{R}\right)\right] & \text{for } k = j, \\ \dfrac{aR}{\varepsilon_{nj}^2 - \varepsilon_{nk}^2}\left[\varepsilon_{nk}\mathrm{J}_n\left(\dfrac{\varepsilon_{nj}a}{R}\right)\mathrm{J}'_n\left(\dfrac{\varepsilon_{nk}a}{R}\right) - \varepsilon_{nj}\mathrm{J}_n\left(\dfrac{\varepsilon_{nk}a}{R}\right)\mathrm{J}'_n\left(\dfrac{\varepsilon_{nj}a}{R}\right)\right] & \text{for } k \neq j, \end{cases} \tag{A.2}$$

$$\beta_{nmj} = \int_a^R W_{nm}(r)\mathrm{J}_n\left(\frac{\varepsilon_{nj}r}{R}\right)r\,\mathrm{d}r = A_{nm}[\beta_{Jnmj} + B_{nm}\beta_{Inmj} + C_{nm}\beta_{Knmj} + D_{nm}\beta_{Ynmj}], \tag{A.3}$$

where

$$\beta_{\mathrm{J}nmj} = \int_a^R \mathrm{J}_n\left(\frac{\lambda_{nm}r}{R}\right)\mathrm{J}_n\left(\frac{\varepsilon_{nj}r}{R}\right)r\,\mathrm{d}r = \frac{R}{\lambda_{nm}^2 - \varepsilon_{nj}^2}\left[-R\lambda_{nm}\mathrm{J}_n(\varepsilon_{nj})\mathrm{J}'_n(\lambda_{nm}) - a\left\{\varepsilon_{nj}\mathrm{J}_n\left(\frac{\lambda_{nm}a}{R}\right)\mathrm{J}'_n\left(\frac{\varepsilon_{nj}a}{R}\right) - \lambda_{nm}\mathrm{J}_n\left(\frac{\varepsilon_{nj}a}{R}\right)\mathrm{J}'_n\left(\frac{\lambda_{nm}a}{R}\right)\right\}\right], \tag{A.4}$$

$$\beta_{\mathrm{I}nmj} = \int_a^R \mathrm{I}_n\left(\frac{\lambda_{nm}r}{R}\right)\mathrm{J}_n\left(\frac{\varepsilon_{nj}r}{R}\right)r\,\mathrm{d}r = \frac{R}{\lambda_{nm}^2 + \varepsilon_{nj}^2}\left[\lambda_{nm}R\mathrm{J}_n(\varepsilon_{nj})\mathrm{I}'_n(\lambda_{nm}) - a\left\{\lambda_{nm}\mathrm{J}_n\left(\frac{\varepsilon_{nj}a}{R}\right)\mathrm{I}'_n\left(\frac{\lambda_{nm}a}{R}\right) - \varepsilon_{nj}\mathrm{I}_n\left(\frac{\lambda_{nm}a}{R}\right)\mathrm{J}'_n\left(\frac{\varepsilon_{nj}a}{R}\right)\right\}\right], \tag{A.5}$$

$$\beta_{\mathrm{Y}nmj} = \int_a^R \mathrm{Y}_n\left(\frac{\lambda_{nm}r}{R}\right)\mathrm{J}_n\left(\frac{\varepsilon_{nj}r}{R}\right)r\,\mathrm{d}r = \frac{R}{\lambda_{nm}^2 - \varepsilon_{nj}^2}\left[-R\lambda_{nm}\mathrm{J}_n(\varepsilon_{nj})\,Y'_n(\lambda_{nm}) - a\left\{\varepsilon_{nj}\,Y_n\left(\frac{\lambda_{nm}a}{R}\right)\mathrm{J}'_n\left(\frac{\varepsilon_{nj}a}{R}\right) - \lambda_{nm}\mathrm{J}_n\left(\frac{\varepsilon_{nj}a}{R}\right)Y'_n\left(\frac{\lambda_{nm}a}{R}\right)\right\}\right], \tag{A.6}$$

$$\beta_{\mathrm{K}nmj} = \int_a^R \mathrm{K}_n\left(\frac{\lambda_{nm}r}{R}\right)\mathrm{J}_n\left(\frac{\varepsilon_{nj}r}{R}\right)r\,\mathrm{d}r = \frac{R}{\lambda_{nm}^2 + \varepsilon_{nj}^2}\left[\lambda_{nm}R\mathrm{J}_n(\varepsilon_{nj})\mathrm{K}'_n(\lambda_{nm}) - a\left\{\lambda_{nm}\mathrm{J}_n\left(\frac{\varepsilon_{nj}a}{R}\right)\mathrm{K}'_n\left(\frac{\lambda_{nm}a}{R}\right) - \varepsilon_{nj}\mathrm{K}_n\left(\frac{\lambda_{nm}a}{R}\right)\mathrm{J}'_n\left(\frac{\varepsilon_{nj}a}{R}\right)\right\}\right]. \tag{A.7}$$

The coefficients γ_{0m} and η_{0k} in Eq. (23) are as follows:

$$\gamma_{0m} = \int_a^R W_{0m}(r)r\,\mathrm{d}r = A_{nm}\left[\gamma_{\mathrm{J}0m} + B_{0m}\gamma_{\mathrm{I}0m} + C_{0m}\gamma_{\mathrm{Y}0m} + D_{0m}\gamma_{\mathrm{K}0m}\right], \tag{A.8}$$

where

$$\gamma_{\mathrm{J}0m} = \int_a^R \mathrm{J}_0\left(\frac{\lambda_{0m} r}{R}\right) r\,\mathrm{d}r = \frac{R}{\lambda_{0m}}\left[R\mathrm{J}_1(\lambda_{0m}) - a\mathrm{J}_1\left(\frac{\lambda_{0m} a}{R}\right)\right], \tag{A.9}$$

$$\gamma_{\mathrm{I}0m} = \int_a^R \mathrm{I}_0\left(\frac{\lambda_{0m} r}{R}\right) r\,\mathrm{d}r = \frac{R}{\lambda_{0m}}\left[R\mathrm{I}_1(\lambda_{0m}) - a\mathrm{I}_1\left(\frac{\lambda_{0m} a}{R}\right)\right], \tag{A.10}$$

$$\gamma_{\mathrm{J}0m} = \int_a^R \mathrm{J}_0\left(\frac{\lambda_{0m} r}{R}\right) r\,\mathrm{d}r = \frac{R}{\lambda_{0m}}\left[R\mathrm{J}_1(\lambda_{0m}) - a\mathrm{J}_1\left(\frac{\lambda_{0m} a}{R}\right)\right], \tag{A.11}$$

$$\gamma_{\mathrm{K}0m} = \int_a^R \mathrm{K}_0\left(\frac{\lambda_{0m} r}{R}\right) r\,\mathrm{d}r = \frac{R}{\lambda_{0m}}\left[-R\mathrm{K}_1(\lambda_{0m}) + a\mathrm{K}_1\left(\frac{\lambda_{0m} a}{R}\right)\right], \tag{A.12}$$

$$\eta_{0k} = \int_0^a \mathrm{J}_0\left(\frac{\varepsilon_{0k} r}{R}\right) r\,\mathrm{d}r = \frac{aR}{\varepsilon_{0k}}\mathrm{J}_1\left(\frac{\varepsilon_{0k} a}{R}\right). \tag{A.13}$$

References

[1] M.K. Kwak, Vibration of circular plates in contact with water, *Journal of Applied Mechanics* 58 (1991) 480–483.
[2] M. Amabili, G. Dalpiaz, C. Santolini, Free-edge circular plates vibrating in water, *Modal Analysis* 10 (1995) 187–202.
[3] M. Amabili, M.K. Kwak, Vibration of circular plates on a free fluid surface: effect of surface waves, *Journal of Sound and Vibration* 226 (1999) 407–424.
[4] M. Amabili, G. Frosali, M.K. Kwak, Free vibrations of annular plates coupled with fluids, *Journal of Sound and Vibration* 191 (1996) 825–846.
[5] C.-C. Liang, Y.-S. Tai, P.-L. Li, Natural frequencies of annular plates contact with fluid, *Journal of Sound and Vibration* 228 (1999) 1167–1181.
[6] H.F. Bauer, Coupled frequencies of a liquid in a circular cylindrical container with elastic liquid surface cover, *Journal of Sound and Vibration* 180 (1995) 689–704.
[7] H.F. Bauer, M. Chiba, Hydroelastic viscous oscillations in a circular cylindrical container with an elastic cover, *Journal of Fluids Structures* 14 (2000) 917–936.
[8] M. Amabili, Vibrations of circular plates resting on a sloshing liquid: solution of the fully coupled problem, *Journal of Sound and Vibration* 245 (2001) 261–283.
[9] F. Welt, V.J. Modi, Vibration damping through liquid sloshing, Part I: a nonlinear analysis, *Journal of Vibration and Acoustics* 114 (1992) 10–16.
[10] F. Welt, V.J. Modi, Vibration damping through liquid sloshing, Part II: experimental results, *Journal of Vibration and Acoustics* 114 (1992) 10–16.
[11] R.J. Hung, H.L. Pan, Baffle effect on sloshing-modulated torques responsed to orbital accelerations in microgravity, *Journal of Spacecraft and Rockets* 32 (1995) 723–731.
[12] R. Sharma, S.E. Semercigil, O.F. Turan, Floating and immersed plates to control sloshing in a cylindrical container at the fundamental mode, *Journal of Sound and Vibration* 155 (1992) 365–370.
[13] H.F. Bauer, W. Eidel, Frictionless liquid sloshing in circular cylindrical container configurations, *Aerospace Science and Technology* 3 (1999) 301–311.
[14] H.F. Bauer, K. Komatsu, Coupled frequencies of a frictionless liquid in a circular cylindrical tank with an elastic partial surface cover, *Journal of Sound and Vibration* 230 (2000) 1147–1163.
[15] A. Gedikli, M.E. Erguven, Seismic analysis of a liquid storage tank with a baffle, *Journal of Sound and Vibration* 223 (1999) 141–155.

[16] X. Gou, T. Li, X. Ma, B. Wang, H. Haung, Synchronous Hopf-bifurcation and damping osmosis phenomena of liquid–spacecraft coupled system, *American Institute of Aeronautics and Astronautics Journal* 39 (2001) 225–232.
[17] J.R. Cho, H.W. Lee, K.W. Kim, Free vibration analysis of baffled liquid-storage tanks by the structural-acoustic finite element formulation, *Journal of Sound and Vibration* 258 (2002) 847–866.
[18] K.C. Biswal, S.K. Bhattacharyya, P.K. Sinha, Free-vibration analysis of liquid-filled tank with baffles, *Journal of Sound and Vibration* 259 (2003) 177–192.
[19] ANSYS User's Manual, Revision 5.6, Swanson Analysis System Inc., Houston, PA, USA, 1999.